Influence of minibasin obstruction on canopy dynamics in the northern Gulf of Mexico

Naiara Fernandez*, Oliver B. Duffy, Frank Peel, Michael R. Hudec

Bureau of Economic Geology, Jackson School of Geosciences, The University of Texas at Austin, University Station, Box X, Austin, Texas, 78713-8924, USA

**Corresponding author: naiara.fernandez@beg.utexas.edu*

Abstract

In salt-detached gravity-gliding/spreading systems the detachment geometry is a key control on the downslope mobility of the supra-salt sequence. Here we used regional 3D seismic data to examine a salt-stock canopy in the northern Gulf of Mexico slope, in an area where supra-canopy minibasins subsided vertically and translated downslope above a complex base-of-salt. If thick enough, minibasins can interact with, and weld to, the base-of-salt and be obstructed from translating downslope. Based on the regional maps of the base of allochthonous salt and the base of the supra-canopy sequence, the key controls on minibasin obstruction, we distinguished two structural domains in the study area: a highly obstructed domain and a highly mobile domain. Large-scale translation of the supra-canopy sequence is recorded in the mobile domain by a far-travelled minibasin and a ramp syncline basin. These two structures suggest downslope translation on the order of 40 km from Plio-Pleistocene to Present. In contrast, translation was impeded in the obstructed domain due to supra-canopy bucket minibasins subsiding into feeders during the Pleistocene. As a result, we infer that differential translation occurred between the two domains and argue that a deformation area between two differentially translating supra-canopy minibasin domains is difficult to recognize. However, characterizing domains according to base-of-salt geometry and supra-canopy minibasin configuration can be helpful in identifying domains that may share similar subsidence and downslope translation histories.

Introduction

In passive-margin salt basins, a regional slope facilitates the formation of salt-detached gravity-gliding/spreading systems (Cobbold and Szatmari, 1991; Jackson et al., 1994; Schultz-Ela, 2001; Hudec and Jackson, 2004; Brun and Fort, 2004, 2011; Peel, 2014). If a homogeneous sedimentary cover detaches over a smooth base-of-salt, kinematically linked domains of upslope extension and downslope shortening develop (e.g. Cobbold and Szatmari, 1991; Brun and Fort 2004, 2011; Hudec and Jackson, 2004; Rowan et al., 2004). However, in areas where the translation occurs above a high-relief base-of-salt, strain patterns are more complex (e.g. Gaullier et al., 1993; Loncke et al., 2006; Dooley et al., 2017a, b; 2018; Pichel et al., 2019a,b).

Kinematically linked systems also occur above allochthonous salt canopies. However, strain patterns above salt canopies can be complicated largely due to interactions between the supra-canopy minibasins and the extreme relief on the base-of-salt (e.g. Krueger, 2010; Duffy et al. 2019). Duffy et al. (2019) present an example from the mid-to-lower slope of the northern Gulf of Mexico, a setting characterized by a high-relief base-of-salt overlain by a heterogeneous system of supra-canopy minibasins. The authors propose that as minibasins subsided into the canopy, they also translated downslope. Thus, when minibasins are thick enough, they can weld against the high-relief base-of-salt and become obstructed from freely translating downslope. Importantly, minibasins can be obstructed to different degrees depending on the weld geometry. For example, severely-obstructed minibasins (e.g. minibasins welded laterally against vertical feeder walls, also known as bucket minibasins) may cease translating completely, whereas mildly-obstructed minibasins may simply slow down (Duffy et al., 2019). As the downslope flow of salt and the supra-canopy sequence continues around obstructed minibasins the local strain field is modified, with zones of shortening typically developing immediately upslope of the obstructed minibasins, and extensional breakaways immediately downslope (Krueger, 2010; Duffy et al., 2019).

An implication of the minibasin obstruction model is that adjacent minibasins on the slope can be obstructed to different degrees, and thus differential degrees of downslope translation can occur. The differential translation of variably obstructed

minibasins should be accommodated by 3D strains and strike-slip deformation (Rowan et al., 1999; Krueger, 2010; Duffy et al., 2019), however, such deformation can be difficult to recognize in salt-detached systems. Critically, it is unknown how important the principles of minibasin obstruction are at larger scales. For example, can entire portions or domains of supra-canopy sequence be variably obstructed and influence the dynamics of salt-canopy advance? Furthermore, if differential translation occurs between minibasin domains, can we identify the structures that accommodate that deformation? Characterizing domains according to the structural configuration of minibasin obstructing elements can be helpful in identifying areas where minibasins may share similar subsidence and downslope translation stories, which is ultimately useful for basin structural and depositional reconstructions through time and for regional strain analyses.

Here, we apply the minibasin obstruction model to an area containing numerous minibasins that are subsiding into a salt canopy and that are translating downslope above a high-relief base-of-salt. First, we examine the morphology of the base-of salt and the configuration of overlying supra-canopy minibasins. We couple this with observations of the structural styles observed in downslope oriented seismic cross-sections to constrain the style and degree of minibasin obstruction across the study area. Based on the spatial distribution of minibasin obstruction, we then define two broad domains with different potential for downslope translation and mobility: 1) a highly-mobile unobstructed domain and 2) a highly-obstructed domain. Second, we document and describe striking evidence for large-magnitude downslope translation in the highly-mobile domain (a ramp syncline basin and a far-travelled minibasin) that have not been recognized in the obstructed domain. Third, we describe the area that accommodates the differential translation between the two domains, and discuss the implications of the timing of differential translation on the mappability of such an area.

Data and Methods

The study area is located in the northern Gulf of Mexico in the mid-to-lower slope (Fig. 1). We focus on an area of 13,100 km^2 covered by two 3D pre-stack, depth-migrated, seismic reflection surveys that image to 18 km depth. The seismic data are presented

such that a downward increase in acoustic impedance is marked by a peak (black on seismic sections).

The seismic data was provided by WesternGeco Multiclient and CGG and are commercially sensitive, so the precise geographic location cannot be released. All maps are rotated, and for the ease of description, any geographical cardinal references within this work are given in the framework of an arbitrarily defined “North”. Location of seismic sections cannot be released, neither the absolute depth of sections. However, the basinward direction is indicated in the sections, all of which have a coarsely “NW”-“SE” orientation (with respect to the arbitrary “North”).

Three surfaces have been mapped in the study area: the base Sigsbee canopy, the top Sigsbee canopy, and the seabed (Fig. 2). Of these surfaces, the deepest is the base Sigsbee canopy (sometimes referred to as base-of-salt in the text), a composite surface that for the most part corresponds to the top of the primary sedimentary sequence or top primary minibasin (*sensu* Pilcher et al., 2011). Although the overall seismic quality is good, the data contains some shadow areas and data-wipeout zones at depth that require a careful interpretation of the base Sigsbee canopy. We have followed the guidelines provided by Jackson and Hudec (2017) in order to avoid common pitfalls of base-of-salt interpretation. This is especially important when interpreting feeders in the study area. Where feeders are present, the base Sigsbee canopy surface extends down the feeders and includes their flanks as well as their base, that corresponds to the deep salt level (autochthonous or parautochthonous salt) (Fig. 2). The top Sigsbee canopy surface (sometimes referred to as top-of-salt in the text), corresponds to the base of the supra-canopy sedimentary sequence and thus, highlights the geometry of the supra-canopy minibasins (Fig. 2). We used the base-of-salt and top-of-salt horizons to calculate the thickness of the supra-canopy sedimentary sequence. Due to the relatively low amplitude relief of the seafloor compared to the top Sigsbee canopy, the supra-canopy thickness map reproduces the geometric configuration of the top Sigsbee canopy (top-of-salt) horizon. For consistency, we refer to the top Sigsbee canopy horizon, instead of the thickness map, to describe and discuss the supra-canopy minibasin configuration (Fig. 2). Where available, surface picks based on biostratigraphic markers from BOEM well-data were used to assign an age to the interpreted horizons.

Geological Context and Structural Elements

The Gulf of Mexico started opening when South America moved away from North America, during the breakup of Pangea in the Late Triassic (e.g. Pindell and Dewey, 1982; Salvador, 1991). The basin continued growing during a second phase of rifting, when the Yucatan block moved away from North America during Late Jurassic (e.g. Pindell and Dewey, 1982; Salvador, 1991). Deposition of Jurassic Louann salt occurred when the Gulf of Mexico basin was isolated from greater ocean circulation during rifting (e.g. Salvador, 1987). The Louann salt is variable in thickness, reflecting the rift-related topography, and is absent over most of the oceanic crust in the central parts of the Gulf of Mexico (e.g. Worral and Snelson, 1989; Sawyer et al., 1991; Peel et al., 1995; Hudec et al., 2013; Pindell et al., 2014, 2018; Curry et al., 2018; Rowan, 2014, 2018). In the northern Gulf of Mexico, salt was loaded by sediments and probably mobilized since Late Jurassic (e.g. Nettleton, 1955; Peel et al., 1995; Rowan et al., 1995), when deposition was dominated by marine carbonates, with localized clastic inputs (e.g. Salvador, 1987, 1991; Galloway et al., 1991; Galloway, 2008). During the Cenozoic, large volumes of clastic sediments were deposited in the Northern Gulf of Mexico, which forced the shelf margin to prograde hundreds of kilometers (e.g. Galloway et al., 1991; Galloway, 2008). The loaded autochthonous salt was able to flow into diapirs that rose thorough the primary stratigraphic sequence so that salt was emplaced onto higher stratigraphic levels forming allochthonous salt sheets. The Sigsbee Salt Canopy was formed through coalescence of many of these salt sheets (e.g. Wu et al., 1990b; Peel et al., 1995; Diegel et al., 1995; Rowan et al., 1995). Neogene to Recent sediments have been deposited on top of the Sigsbee canopy, forming secondary or supra-canopy minibasins (e.g. Worral and Snelson, 1989; Wu et al., 1990a, b; Diegel et al., 1995; Peel et al., 1995, Pilcher et al., 2011). As the canopy salt flowed downslope assisted by gravity, so did the supra-canopy minibasins. Minibasins were thus translating downslope at the same time as they were subsiding into the salt.

The bathymetry map of the northern Gulf of Mexico (Fig. 1) illustrates the location and extent of the Sigsbee Canopy. The Sigsbee canopy is located basinwards of the shelf edge (Fig. 1). Here, the nature of the seafloor is rugose with numerous topographic lows,

each of which corresponds to a supra-canopy minibasin. The Sigsbee Escarpment is the prominent topographic feature that marks the basinward limit of the salt canopy (Fig. 1).

In the study area, the two levels of salt can be observed in a seismic section oriented along strike of the slope (Fig. 2). The deepest level of salt corresponds to the autochthonous Louann salt (the stratigraphic level) but can, in places, also correspond to parautochthonous salt extruded on top of crust being created or exhumed during the opening of the Gulf of Mexico (e.g. Sawyer et al., 1991; Peel et al., 1995; Hudec et al., 2013; Norton et al., 2016). In most cases, the Louann salt has been completely evacuated from this deep level and only welds remain. The shallow level of salt corresponds to the Sigsbee salt canopy. Salt feeders are the diapirs through which salt moved from its source layer to "feed" the allochthonous salt sheets. Due to shortening, feeders may be closed, with the walls of the feeders welded against each other. Where the feeders remain open, they may be filled with supra-canopy minibasins.

Morphology of Base Sigsbee Canopy and Supra-Canopy Minibasins

Two key elements must be considered for assessing the potential for minibasin obstruction to occur: 1) the relief of the base Sigsbee Canopy (base-of-salt); and 2) the thickness of supra-canopy minibasins (configuration of the top Sigsbee Canopy or top-of-salt horizon). When the configuration of these two elements allows for welding of a minibasin, minibasin obstruction can occur. We will describe these two key elements in the study area.

Base Sigsbee Canopy Relief

The base Sigsbee Canopy surface is highly rugose with relief exceeding 15 km in some areas (Fig. 3a). Feeders connecting the deep salt level or equivalent weld with the shallow salt are clearly visible on the mapped surface as sub-circular to elliptical low areas bounded by vertical to sub-vertical walls that are 7-8 km tall (Fig. 3a). Feeder diameters are in the range of 10 to 15 km but there are few instances of elongated feeders that are 30 km long. Although the negative relief represented by feeders is remarkable, feeders are not the only elements that influence the topography of the surface. The morphology of the top primary basins also influences the overall relief of the base Sigsbee canopy. The top of the sub-canopy basins varies from being smooth and almost flat in some areas,

to being highly rugose in areas, with localized positive relief in the form of protrusions and narrow ridges (Fig. 3a).

Supra-Canopy Minibasin Configuration

The structure map of the top Sigsbee canopy (top-of-salt) corresponds to the base of the supra-canopy minibasins (Fig. 3b). As such, the surface illustrates the geometry and configuration of the supra-canopy minibasins. Minibasins are expressed as topographic lows that are sub-circular, elliptical or highly irregular in shape. Over 50 minibasins are present in the study area, with thicknesses ranging between 2 km to 13 km. Minibasins are bounded by an irregular network of salt massifs and walls (topographic highs in the structure map) (Fig. 3b). Typically, supra-canopy minibasins are surrounded by salt at deep levels, whereas at shallower levels, they are yoked together by sediment beams (Fig. 2).

Spatial Variations in Minibasin Obstruction Styles

Having established that minibasin obstruction is primarily controlled by the relationship between the base-of-salt surface and the configuration of the overlying supra-canopy minibasins, and having described these two elements in our study area, we now examine the spatial distribution of obstructed minibasins. Both the base-of-salt relief and the minibasin configuration are variable across the study area and we use these variations to classify two domains: the “Northeast” and “Southwest” domains. Seismic sections oriented roughly parallel to the downslope translation direction (Fig. 4 and 5) highlight key differences between these two domains (exact line locations are withheld for data confidentiality reasons).

Structural Style of the “Southwest” Domain

Feeders are more abundant and are generally larger and deeper in the “Southwest” compared to the “Northeast” (Fig. 3a). Also, in the “Southwest”, areas between feeders exhibit higher topographic relief, with more positive relief features such as ridges, resulting in a highly rugose form (Fig. 3a). In general, the domain shows a high-relief base-of-salt with a well-developed egg-crate-like morphology that is not present in

208 the “Northeast”. In addition, thicker minibasins are more common in the “Southwest” than
209 in the “Northeast” (Fig. 3b).
210 Two seismic cross sections from the “Southwest” highlight the interaction between
211 the high relief base-of-salt and the thicker minibasins (Fig. 4). One of the seismic sections
212 represents an area with abundant feeders (Fig. 4a), whereas the other shows only two
213 feeders, one of which is welded shut (Fig.4b). The base Sigsbee Canopy is not flat, with
214 many local highs and steep zones (Fig. 4b). In both seismic sections, supra-canopy
215 minibasins are welded at their base or at the flanks on top of primary basins or in contact
216 with feeder flanks. In fact, all feeders in the seismic section contain minibasins that have
217 sunk into the feeders to varying degrees (bucket minibasins). A minibasin may sink all the
218 way down into the feeder and weld at their base at the deep salt level (see example in
219 Figs. 4a and b). Alternatively, minibasins may sink only partway into the feeder. Several
220 examples of minibasins partially sunk into the feeder are present in the seismic section
221 (minibasins denoted “a”, “b” and “c”; Fig. 4a). Thus, the “Southwest” domain is not only
222 characterized by the presence of abundant wide feeders, but also by the fact that in most
223 cases these feeders are filled with bucket minibasins (Fig. 4a and 6a).
224
225 ## Structural Style of the “Northeast” Domain
226 Overall, there are fewer identified feeders in the “Northeast” domain, and they are
227 smaller and narrower than the ones in the “Southwest” (Fig. 3a). Areas surrounding the
228 feeders in the “Northeast” exhibit a relatively smooth and flat topography with limited relief
229 on base Sigsbee Canopy surface (Fig. 3a). Furthermore, minibasins in the “Northeast”
230 domain are generally thinner and shallower, and more frequently closely clustered or
231 connected through sediment beams than in the “Southwest” (Fig. 3b).
232 Two seismic sections from the “Northeast” illustrate the relationships between the
233 supra-canopy minibasins and the base-of-salt (Figs 5a and b). In some areas, the base
234 Sigsbee Canopy surface is very continuous and not disrupted by any feeders (Fig. 5a),
235 whereas in other areas feeders are present, but they are surrounded by a relatively
236 smooth base-of-salt (Fig. 5b). The overlying minibasins are welded against a smooth or
237 gently dipping base-of-salt (Fig. 5a), or alternatively, the minibasins are not thick enough
238 to be welded to the base-of-salt (Fig. 5b). In any case, the supra-canopy minibasins in

the “Northeast” domain are not thick enough to have completely sank into the feeders (Fig. 5b). In summary, the “Northeast” domain shows fewer and smaller feeders than the “Southwest”, with no bucket minibasins developed (Fig. 5 and 6a).

Differential Potential Mobility of the “Southwest” and “Northeast” Domains

Given that the “Northeast” domain contains fewer highly-to-severely obstructed minibasins than the “Southwest” domain (Fig. 6b), it is likely to have higher degree of mobility, compared to the severely-obstructed supra-canopy sequence in the “Southwest” domain (Fig. 7a). Structural styles and potential mobility of the two domains are represented by the synoptic sections presented in Figs. 7b, c and d.

Evidence for large-magnitude downslope translation in the ‘Northeast’ Domain

The mid-to-lower slope of the northern Gulf of Mexico is a translational domain of a salt-detached gravity-gliding system. Estimating the magnitude of translation in the translational domain is difficult for two reasons. First, due to the heterogeneously thick cover sequence where minibasins are abundant, clear structural indicators of movement such as fault cutoffs are not common (Jackson and Hudec, 2005). Second, as described in Duffy et al., 2019, strain patterns in the translational domain can be extremely complex, with localized areas of shortening and extension surrounding obstructed minibasins. Two lines of evidence can be used to constrain the amount of translation of the supra-canopy sequences within the translational domain: 1) rafted blocks or far-travelled minibasins (e.g. Jackson et al., 2010, Fiduk et al., 2014) and 2) salt-detached ramp synclines (herein termed RSBs, Pichel et al., 2018) (e.g. Jackson and Hudec, 2005) (Fig. 8). Here we provide examples of each of these structures to constrain the amount of down-slope translation of the supra-canopy sequence in the study area.

Far-travelled minibasins

Transported or rafted sediment packages, including entire minibasins and carapace blocks, can provide estimates of translation magnitude if the upslope location

where the package originated can be identified (e.g. Jackson et al., 2010) (Fig. 8a). As it moves downslope, extruded salt can transport supra-salt stratal packages (e.g. carapace sections of up to 25 km-wide and up to few kilometers in thickness; Hart et al. 2004). Rafted blocks have been documented across the northern Gulf of Mexico (e.g. Jackson et al., 2010; Pilcher et al., 2014, Fiduk et al., 2014). Rafted carapace blocks containing Mesozoic-age carbonates could have travelled tens of kilometers (>100 km) away from the salt structure on which they were originally deposited as roof material (Fiduk et al., 2014).

In some instances, transported supra-salt stratal packages are entire minibasins that contain stratigraphic duplicates of the subsalt sedimentary sections that lie below them (e.g. Mount et al., 2006; Jackson et al., 2010) (Fig. 8b). If an entire minibasin was transported by salt, it must have left a “gap” or “hole” in the subsalt stratigraphic sequence big enough to fit the entire transported stratigraphic package. Identifying the source area of a specific transported stratal package can provide insights into lateral transport magnitudes as well as minimum required salt thickness (Jackson et al., 2010).

In the “Northeast” domain, we have identified three minibasins that contain a stratigraphic sequence of Mesozoic to Miocene age and that are structurally on top of a sub-canopy primary sequence of Mesozoic to Miocene age. The duplication of Mesozoic to Miocene section in a supra-canopy minibasin implies that the minibasin must have originated somewhere upslope of its current position. The biggest of these three minibasins contains over 3500 meters of duplicated stratigraphic sequence with an area of 12 x 13 kilometers (Fig. 9). The other two minibasins contain around 2000 meters of duplicated sequence and they are smaller in extent. Upslope of these three minibasins there are few areas from where the sub-canopy Mesozoic to Miocene stratigraphic sequence is missing (feeders) that are big enough to fit these minibasins. The nearest potential source area from where the minibasin with the thickest duplicated stratigraphic section could have originated corresponds to a large feeder located up-slope (Fig. 9). The distance from the minibasin to this potential source area is around 40 km. This implies that the minibasin was rafted at least 40 km downslope from its source area. Presumably, the minibasin was thinner when it was uplifted from its source area and it became thicker as it translated downslope.

Salt-detached ramp syncline basin

Salt-detached RSB's are growth synclines that form by translation of the sedimentary cover above a stepped salt detachment (e.g. Jackson and Hudec, 2005) (Fig. 8c). Salt-detached ramp syncline basins were first recognized as indicators of the translation of the sedimentary cover in the Kwanza Basin, Angola (Marton et al., 1998; Peel et al., 1998 and Spencer et al., 1998). Identification and description of RSBs in other places have provided insights into the evolution of salt-bearing basins such as the Santos and Campos Basins in Brazil (e.g. Dooley et al. 2016; Pichel et al., 2018) and the Red Sea (e.g. Rowan, 2014) for example. Assuming the underlying ramp was fixed, the distance between the top of the ramp and a given onlap point records the translation distance since the deposition time of the horizon forming the onlap (Jackson & Hudec, 2005) (Fig. 8c).

In the "Northeast" domain, in an area of relatively low topographic relief of the sub-canopy section, we have identified a structure that we interpret as an RSB (Fig. 10). The base Sigsbee Canopy has a gentle landward slope for several tens of kilometers, with steeper seaward-dipping slope landward (the ramp). The supra-canopy section above the ramp-to-flat transition has a basal and, for most of the part, constant-thickness sequence, that we interpret as a prekinematic preramp wedge (Fig. 10). The overlying sedimentary sequence (Fig. 10), has a basal isopach thick on top of the basinward edge of the pre-ramp sequence. The overlying isopach thicks have their depocenters successively shifted landward with respect to the underlying one forming a characteristic RSB geometry. An onlap surface separates the RSB and underlying pre-wedge sequence. The horizontal distance between the edge of the ramp and the onlap point of the oldest isopach thick on top of the pre-ramp wedge is ~40 km. The sub-canopy ramp is not completely imaged within the seismic data and therefore the position of the transition from the ramp to the landward flat is not exactly known. Thus, ~40 km is the minimum downslope translation that occurred from the time the lowermost isopach thick was deposited. This magnitude is similar to the translation estimated for the far-travelled minibasin.

Timing of translation and obstruction

Synoptic cross sections help illustrate the evolution of the two domains (Fig. 11). In an early stage, because the supra-canopy minibasins are thin, they freely move downslope, regardless of the underlying geometry of the base-of-salt relief (Fig. 11a). However, as the minibasins translate downslope they become thicker. In the “Southwest” Domain, where the bigger feeders are present, supra-canopy minibasins can experience an increased subsidence as they pass over feeders containing thick salt where salt evacuation is easier. Subsequently, minibasin subsidence is fixed in place over the feeder and forms a bucket minibasin (Fig.11b). Bucket minibasins are welded to the feeder walls and thus are severely obstructed (Fig.11b). The severe obstruction impedes further minibasin translation and creates the characteristic upslope shortening and downslope extension strain pattern described by Duffy et al. (2019) (represented in Fig. 11b and c). In the “Northeast” Domain instead, the smoother base of salt relieve does not enable the formation of bucket minibasins and thus, the supra-canopy minibasins can continue their downslope translation (Fig.11b). The different degree of obstruction results in differential advance of the supra-canopy cover that is accommodated in between the two domains (Fig. 11c). But when was the “Southwest” Domain obstructed, and the differential translation accommodated?

According to our interpretation of the seismic and available age constraints from well data, sometime during the Upper Miocene to Pliocene, the far-travelled minibasin (Fig. 9), was lifted from its source diapir because salt in the diapir was actively rising. At that time, the minibasin was probably thinner than at present day, thus it was easier to lift it out of the diapir. After being lifted, the minibasin started its downslope translation leaving behind an unroofed diapir and becoming thicker during its downslope translation as new sediments were accumulated on top. At present, this source-diapir contains a bucket minibasin (Fig. 9). It is not possible to know exactly how far upslope from the feeder the bucket minibasin formed or nucleated. Considering our own translation estimates for the “Northeast” domain as well as existing estimates in other areas of the northern Gulf of Mexico (e.g. Fiduk et al., 2014), the translation of these minibasins could have been in the order of few-tens of kilometers. However, interpreted stratal geometries and available age constraints indicate a transition to a wedge-shaped stratigraphic package (increased

asymmetric subsidence) of the bucket minibasin at around the Plio-Pleistocene marker (Fig. 9). Based on this interpretation, we suggest that the minibasin was translated over and subsided into the feeder during the Plio-Pleistocene to Early Pleistocene (ca. 2.30-1.39 Ma) (Fig. 9). The down-dip time-equivalent of the wedge-shaped sequence in the bucket-minibasin corresponds to a constant-thickness sequence in several other minibasins (including the far-travelled minibasin). Due to the increased subsidence, the minibasin became "trapped" into the feeder and was therefore severely-obstructed from translating downslope. Subsequent subsidence (Pleistocene, after 1.39 Ma) occurred as it sank further into the feeder. Directly down-dip of the bucket minibasin, an area of extension accommodated the differential translation between the obstructed bucket minibasin (effectively locked) and the down-dip minibasins (e.g. Duffy et al., 2019) (Fig. 9) within the mobile domain. In the "Southwest" domain, there are other instances of bucket-minibasins completely filling the feeders (Fig. 6a). Limited available age data suggests that at least one other bucket minibasin was probably in its present position, above the feeder, by mid-Pleistocene (before 1.39 Ma). Thus, we suggest that the cover sequence in the "Southwest" domain was probably severely-obstructed by mid-Pleistocene.

In contrast, based on the interpretation of the stratal geometries and available age constraints, the RSB recorded continuous translation from Pliocene or earlier to Present-Day in the "Northeast" domain (Fig. 10). Based on the onlap position of the Plio-Pleistocene (2.30 Ma) marker, the RSB translated at least 5 km farther during that time interval (Fig. 10). Thus, the severe obstruction of the "Southwest" domain and coeval translation of the "Northeast" domain must have resulted in differential translation between the two domains from Pleistocene to Present.

We have mapped the Sigsbee canopy front advance based on the interpretation and mapping of stratigraphic salt-cutoffs in the study area (Fig. 12b). There was differential salt advance of the Sigsbee canopy front during the same time interval when we propose the differential translation between the two domains occurred (Fig. 11c and 12b). As stated by the obstruction model, salt can flow around obstructed minibasins, which is ultimately the reason for the complex strain patterns around minibasins (Krueger, 2010; Duffy et al., 2019). However, assuming that at geological time scales salt behaves

as a fluid of very high viscosity, its resistance to flow around the obstructed (immobile) minibasins is high. Thus, it is harder for salt to flow downslope in the "Southwest" domain were many obstructed/bucket minibasins are present. In contrast, in the "Northeast" domain, salt has less obstacles to flow around. The differential salt advance can be observed in the mapped front of the Sigsbee canopy (Fig. 12b). The amount of differential salt advance is in the order of few kilometers in our study area, similar to the estimated translation of the RSB at the same time interval.

How is Differential Translation between Minibasin Domains Accommodated?

Given the present-day configuration of the two domains in our study area, we have established that they have different potential mobility. We have also suggested, that the "Southwest" domain was obstructed earlier and there has been differential translation between the two domains from Pleistocene to Present. The questions that follow are: is the differential translation reflected in the supra-canopy sequence? Is this differential deformation still active?

Differential translation of supra-canopy sequence should be accommodated by 3D strains and deformation (e.g. Rowan et al., 1999; Krueger, 2010; Pichel et al., 2019a). Differential translation between portions of the supra-canopy sequence have been identified in some areas in the northern Gulf of Mexico, where well-defined strike-slip tear faults accommodate this movement. For example, the submarine Keathley Canyon is located where the Sigsbee Escarpment changes its orientation from a W-E trend to a NW-SE trend (Fig. 1 and 12a). There, a pull-apart basin and associated releasing bends indicate the existence of a long and straight left-lateral strike slip zone following the overall trend of the Keathley Canyon (Fig. 12a) (e.g. Dooley and Schreurs, 2012). This structure has been interpreted as a NW-striking strike-slip zone that separates two structural provinces of the northern Gulf of Mexico with different amounts of translation of the supra-canopy cover. In areas where the base-of-salt is smooth and planar, differential deformation is accommodated by long and linear tear faults (e.g. in areas of the eastern and northern Gulf of Mexico; e.g. Rowan et al., 1999; Krueger, 2010). However, in areas where the supra-canopy minibasins interact with a very irregular base-of-salt canopy and

downslope translating minibasins are obstructed, more complex strain patterns arise (Rowan et al., 1999; Krueger, 2010; Duffy et al., 2019). Differential deformation can be expected to be accommodated in short fault segments bounding minibasins, instead of in long and linear strike-slip faults.

Using seismic data and seafloor bathymetry, we have mapped several seafloor structures in our study area. No long straight right-lateral strike-slip fault spanning across the boundary between the two domains has been identified in the seafloor. Instead, mapped structures correspond to extensional faults with a mainly dip-slip component that bound supra-canopy minibasins that may form conjugate sets with opposite dipping directions defining graben structures (Fig. 12b). In some instances such normal faults are grouped into sets, roughly parallel to the downslope transport direction (Fig. 11b). In many other cases, the groups of normal faults strike perpendicular to the transport direction (Fig. 12b). The latter correspond to extensional breakaways formed immediately downslope of obstructed minibasins (e.g., Duffy et al., 2019). Contractional structures (mainly folds) have been mapped immediately up-dip of one of the severely-obstructed minibasins that lies within a feeder (Duffy et al., 2019). To some degree, the overall distribution of strain on the seafloor across the study area reflects the different structural styles of the two described domains (obstructed vs. non-obstructed). While areas of stretching are widespread across the study area, the identified shortening structures are located in the “Southwest” domain (non-mobile) exclusively (Fig. 12b). In most cases, these areas of shortening correspond to the up-dip shortening associated with obstructed bucket minibasins (Fig. 6 and 12b).

In summary, instead of an easily identifiable zone of localized strike-slip deformation between the two domains of our study area, a complex and diffuse strain pattern with discrete structures distributed along minibasin boundaries is observed in the seafloor. The absence of an area of localized strike slip deformation in the seafloor of the study area can have two interpretations: 1) there is no ongoing differential translation or deformation, or if there is, such deformation is not large enough to create a localized linear strike-slip structure in the seafloor, or 2) differential translation is occurring, but deformation between the two domains is being accommodated in a diffuse way, along minibasin boundaries.

Evidence for earlier stages of differential translation might be even more difficult to identify than in the present-day for three reasons. First, as discussed for the present-day case, earlier differential translation might have been accommodated by a diffuse zone and distributed along minibasin boundaries in several shorter segments. Second, there might have been no supra-canopy sequence deposited in between the minibasins that would have recorded the differential translation, so that deformation would have been accommodated by salt in a cryptic manner. Third, there may have been a supra-canopy sequence that recorded the differential translation, but it was later eroded.

Observations from present-day structures in the seafloor do not show evidence for a localized deformation area between the two described domains. However, the different structural styles of the two domains (obstructed vs. non-obstructed, Fig. 7) are recorded by a characteristic strain pattern distribution in the seafloor (Fig. 12b). While the "Southwest" domain displays complex strain patterns with areas of both shortening and extension related to severely obstructed minibasins, the "Northeast" domain displays dominantly extensional deformation as the supra-canopy sequence translates downslope without severe obstructed processes occurring at present. We argue that the characteristic strain pattern distribution in the seafloor, indicates that the interpreted structural styles (obstructed vs. non-obstructed) are exerting an influence in the present-day deformation of seafloor.

Conclusions

The aim of this study was to investigate if the concept of minibasin obstruction was applicable beyond the scale of individual minibasins. In the study area we distinguished two regional domains based on differences in the base Sigsbee Canopy surface geometry and supra-canopy minibasin thickness, the two key elements in the obstruction process. In the "Southwest" domain, the base-of-salt has high relief with abundant large feeders, filled with thick bucket minibasins that are severely-obstructed from translating downslope. In contrast, the "Northeast" domain is characterized by a base-of-salt that has less relief, sparse and narrow feeders, and few bucket minibasins. We proposed that when large portions of supra-canopy sequence contain multiple severely-obstructed minibasins, each one behaves as a "pin" that "locks" the supra-canopy and sub-canopy

sequences together, and the domain as a whole is severely-obstructed (i.e. the Southwest' domain). In contrast, entire portions of the supra-canopy sequence containing multiple minibasins that are unobstructed or mildly-obstructed are free to translate downslope if the minibasins are too thin or shallow to interact with the base of salt or if the base of salt is relative smooth (i.e. the 'Northeast' domain).

Large-magnitude downslope translation of several tens of kilometers is indicated by two independent structures in the "Northeast" domain, a ramp-syncline and a far-travelled minibasin. Translation of the supra-canopy sequence in the "Northeast" domain seems to have been continuous from at least the early Pleistocene (and probably before) through to the present-day, as recorded by a ramp syncline. In contrast, translation of the supra-canopy sequence in the "Southwest" stopped during the Pleistocene, when several bucket minibasins sank into feeders becoming severely-obstructed. The obstruction of the "Southwest" domain would have resulted in differential translation, with the "Northeast" domain able to translate further.

The deformation zone between differentially translating domains can be difficult to recognize, depending on how such deformation is accommodated. In our study area, seafloor structures suggest complex spatial patterns of local strain segments (extensional breakaways, grabens, thrusts, folds) around minibasins. However, while stretching is the dominant form of deformation across the study area, shortening structures (largely-located immediately updip of severely-obstructed minibasins) are only found within the less-mobile obstructed domain. This observation is in accordance with what the minibasin obstruction model would predict around individual minibasins.

Predictions from the minibasin obstruction model are helpful in making sense of complex strain patterns identified in the seafloor around individual minibasins. Characterizing domains according to base-salt relief, supra-canopy minibasin configuration and mobility potential within a slope setting can be helpful in identifying areas that may share similar subsidence and downslope translation histories. Extending the concepts of obstruction and differential mobility beyond the framework of individual minibasins is thus key in understanding regional dynamics of supra-canopy deformation.

Acknowledgements

We would like to thank Gillian Apps, Chris Jackson and Tim Dooley for scientific discussions and Nancy Cottington for her help with figure drafting. We thank reviewers Scot Krueger, Leonardo Pichel and Sian Evans for their comments which helped improve this work. Thanks to CGG and WesternGeco Multiclient for providing the 3D seismic data and to the Bureau of Ocean Energy Management for seafloor imagery. We also thank the Gulf of Mexico Basin Depositional Synthesis Project (GBDS) at The University of Texas at Austin, specially Craig Fulthorpe, John Virdell and John W. Snedden, for providing the well-data that was used to assign ages to the seismic horizons. The project was funded by the Applied Geodynamics Laboratory (AGL) Industrial Associates program, comprising the following companies: Anadarko, Aramco Services, BHP Billiton, BP, CGG, Chevron, Condor, EcoPetrol, EMGS, ENI, ExxonMobil, Fieldwood, Hess, Ion-GXT, Midland Valley, Murphy, Nexen USA, Noble, Petrobras, Petronas, PGS, Repsol, Rockfield, Shell, Spectrum, Equinor, Stone Energy, TGS, Total, WesternGeco, and Woodside (http://www.beg.utexas.edu/agl/sponsors). The authors received additional support from the Jackson School of Geosciences, The University of Texas at Austin.

References

Brun, J.P. and Fort, X., 2004. Compressional Salt Tectonics (Angolan Margin). Tectonophysics, 382, pp.129-150.

Brun, J.P. and Fort, X., 2011. Salt tectonics at passive margins: Geology versus models. Marine and Petroleum Geology, 28(6), pp.1123-1145.

Cobbold, P.R. and Szatmari, P., 1991. Radial gravitational gliding on passive margins. Tectonophysics, 188(3-4), pp.249-289.

Curry, M. A. E., Peel, F. J., Hudec, M. R., and Norton, I. O., 2018, Extensional models for the development of passive-margin salt basins, with application to the Gulf of Mexico: Basin Research, v. 30, no. 6, p. 1180-1199.

Diegel, F. A., Karlo, J. F., Schuster, D. C., Shoup, R. C., and Tauvers, P. R., 1995, Cenozoic Structural Evolution and Tectono-Stratigraphic Framework of the Northern Gulf Coast Continental Margin, *in* Salt Tectonics: A Global Perspective, *in* Jackson, M. P. A., Roberts, D. G., and Snelson, S., eds., Volume 65, American Association of Petroleum Geologists.

Dooley, T. P., and Schreurs, G., 2012, Analogue modelling of intraplate strike-slip tectonics: A review and new experimental results: Tectonophysics, v. 574-575, p. 1-71.

Dooley, T. P., Hudec, M. R., Carruthers, D., Jackson, M. P. A., and Luo, G., 2017a, The effects of base-salt relief on salt flow and suprasalt deformation patterns — Part 1: Flow across simple steps in the base of salt: Interpretation, v. 5, no. 1, p. SD1-SD23.

Dooley, T. P., Hudec, M. R., 2017b, The effects of base-salt relief on salt flow and suprasalt deformation patterns - Part 2: Application to the eastern Gulf of Mexico, Interpretation, Volume 5, Issue 1

Dooley, T. P., Hudec, M. R., Pichel, L. M., and Jackson, M. P. A., 2018, The impact of base-salt relief on salt flow and suprasalt deformation patterns at the autochthonous, paraautochthonous and allochthonous level: insights from physical models, in McClay, K. R. and Hammerstein, J. A., Passive

Margins: Tectonics, Sedimentation and Magmatism: Geological Society, London, Special Publications, no. 476, 29 p.
Duffy, O. B., Fernandez, N., Peel, F. J., Hudec, M. R., Dooley, T. P., and Jackson, C. A.-L., Obstructed minibasins on a salt-detached slope: An example from above the Sigsbee canopy, northern Gulf of Mexico: Basin Research, v. 0, no. 0.
Fiduk, J. C., Clippard, M., Power, S., Robertson, V., Rodriguez, L., Ajose, O., Fernandez, D., and Smith, D., 2014, Origin, Transportation, and Deformation of Mesozoic Carbonate Rafts in the Northern Gulf of Mexico, Gulf Coast Association of Geological Societies Transactions, Volume 64.
Galloway, W.E., Bebout, D.G., Fisher, W.L., Dunlap, J.B., Jr, Cabrera-Castro, R., Lugo-Rivera, J.E., and Scott, T.M., 1991, Cenozoic. Salvador A. (ed), The Gulf of Mexico basin. The Geology of North America. Geological Society of America, Boulder, Colorado: vol J, pp 245–324
Galloway, W. E., 2008, Chapter 15: Depositional Evolution of the Gulf of Mexico Sedimentary Basin, *in* Miall, A. D., ed., Sedimentary Basins of the World, Volume 5, Elsevier, p. 505-549.
Gaullier, V., Brun, J.P., Gue, G. and Lecanu, H., 1993. Raft tectonics: the effects of residual topography below a salt decollement. Tectonophysics, 228(3-4), pp.363-381.
Hart, W., Jaminski, J., and Albertin, M., 2004, Recognition and Exploration Significance of Supra-Salt Stratal Carapaces *in* Salt Sediment Interactions and Hydrocarbon Prospectivity Concepts, Applications and Case Studies for the 21st Century, *in* Post, P. J., Olson, D. L., Lyons, K. T., Palmes, S. L., Harrison, P. F., and Rosen, N. C., eds., Volume 24, SEPM Society for Sedimentary Geology, p. 0.
Hudec, M. R., and Jackson, M. P. A., 2009, Interaction between spreading salt canopies and their peripheral thrust systems: Journal of Structural Geology, v. 31, no. 10, p. 1114 - 1129.
Hudec, M. R., Norton, I. O., Jackson, M. P., and Peel, F. J., 2013, Jurassic evolution of the Gulf of Mexico salt basin: AAPG bulletin, v. 97, no. 10, p. 1683-1710.
Hudec, M. R., Jackson, M. P., and Peel, F. J., 2013, Influence of deep Louann structure on the evolution of the northern Gulf of MexicoGulf of Mexico Salt Influence: AAPG bulletin, v. 97, no. 10, p. 1711-1735.
Jackson, M.P., Vendeville, B.C. and Schultz-Ela, D.D., 1994. Structural dynamics of salt systems. Annual Review of Earth and Planetary Sciences, 22(1), pp.93-117.
Jackson, M. P. A., and Hudec, M. R., 2005, Stratigraphic record of translation down ramps in a passive-margin salt detachment: Journal of Structural Geology, v. 27, no. 5, p. 889-911.
Jackson, M. P. A., Hudec, M. R., & Dooley, T. P., 2010, Some emerging concepts in salt tectonics in the deepwater Gulf of Mexico: intrusive plumes, canopy-margin thrusts, minibasin triggers and allochthonous fragments. In *Geological Society, London, Petroleum Geology Conference series* (Vol. 7, No. 1, pp. 899-912). Geological Society of London.
Jackson, M. P. A., and Hudec, M. R., 2017, Salt Tectonics: Principles and Practice, Cambridge, Cambridge University Press.
Krueger, S., Dynamics of tear faults in the salt-detached systems of the Gulf of Mexico [abs.], *in* Proceedings AAPG Annual Convention & Exhibition Abstracts2010, Volume 19, p. 137-138.
Marton, G., Tari, G., & Lehmann, C. (1998). Evolution of salt-related structures and their impact on the post-salt petroleum systems of the Lower Congo Basin, offshore Angola. In *American Association of Petroleum Geologists International Conference and Exhibition, Rio de Janeiro. Extended Abstracts Volume* (pp. 834-834).
Mount, V. S., Rodriguez, A., Chaouche, A., Crews, S. G., Gamwell, P., and Montoya, P., 2006, Petroleum system observations and interpretation in the vicinity of the K2/K2-North, Genghis Khan, and Marco Polo fields, Green Canyon, Gulf of Mexico.
Nettleton, L.L., 1955. History of concepts of Gulf Coast salt-dome formation. *AAPG Bulletin*, *39*(12), pp.2373-2383.
Norton, I. O., Carruthers, D. T., and Hudec, M. R., 2016, Rift to drift transition in the South Atlantic salt basins: A new flavor of oceanic crust: Geology, v. 44, no. 1, p. 55-58.
Peel, F. J., Travis, C. J., and Hossack, J. R., 1995, Genetic Structural Provinces and Salt Tectonics of the Cenozoic Offshore U.S. Gulf of Mexico: A Preliminary Analysis, *in* Salt Tectonics: A Global Perspective, *in* Jackson, M. P. A., Roberts, D. G., and Snelson, S., eds., Volume 65, American Association of Petroleum Geologists.
Peel, F., Jackson, M., & Ormerod, D.,1998,. Influence of major steps in the base of salt on the structural style of overlying thin-skinned structures in deep water Angola. In *American Association of Petroleum Geologists International Conference and Exhibition, Rio de Janeiro, Brazil, November, Extended Abstracts Volume* (pp. 366-367).

606 Peel, F.J., 2014. The engines of gravity-driven movement on passive margins: Quantifying the relative
607 contribution of spreading vs. gravity sliding mechanisms. Tectonophysics, 633, pp.126- 142.
608 Pindell, J., and Dewey, J. F., 1982, Permo-Triassic reconstruction of western Pangea and the evolution of
609 the Gulf of Mexico/Caribbean region: Tectonics, v. 1, no. 2, p. 179-211.
610 Pichel, L. M., Peel, F. J., Jackson, C. A. L., and Huuse, M., 2018, Geometry and kinematics of salt-detached
611 ramp syncline basins: Journal of Structural Geology, v. 115, p. 208 - 230.
612 Pichel, LM, A.-L. Jackson, C, Peel, F, Dooley, TP., 2019a, Base-salt relief controls salt-tectonic structural
613 style, São Paulo Plateau, Santos Basin, Brazil. *Basin Res*.; 00: 1– 32
614 Pichel, L.M., Huuse, M., Redfern, J. and Finch, E., 2019b. The influence of base-salt relief, rift topography
615 and regional events on salt tectonics offshore Morocco. *Marine and Petroleum Geology*, *103*, pp.87-
616 113.
617 Pilcher, R. S., Kilsdonk, B., and Trude, J., 2011, Primary basins and their boundaries in the deep-water
618 northern Gulf of Mexico: Origin, trap types, and petroleum system implications: AAPG Bulletin, v. 95,
619 no. 2, p. 219-240.
620 Pilcher, R. S., Murphy, R. T., and McDonough Ciosek, J., 2014, Jurassic raft tectonics in the northeastern
621 Gulf of Mexico: Interpretation, v. 2, no. 4, p. SM39-SM55.
622 Pindell, J., Graham, R., and Horn, B., 2014, Rapid outer marginal collapse at the rift to drift transition of
623 passivemargin evolution, with a Gulf of Mexico case study: Basin Research, v. 26, no. 6, p. 701-725.
624 Pindell, J., Graham, R., and Horn, B. W., 2018, Role of outer marginal collapse on salt deposition in the
625 eastern Gulf of Mexico, Campos and Santos basins: Geological Society, London, Special Publications,
626 v. 476, p. SP476.474.
627 Rowan, 1995, Structural Styles and Evolution of Allochthonous Salt, Central Louisiana Outer Shelf and
628 Upper Slope, in *Jackson MPA, Roberts DG, Snelson S. Salt Tectonics: A Global Perspective*, AAPG
629 Memoir **65,** pp.199-228
630 Rowan, M. G., and Inman, K. F., 2011, Salt-related deformation recorded by allochthonous salt rather than
631 growth strata: Gulf Coast Association of Geological Societies Transactions, v. 61, p. 379-390.
632 Rowan, M. G., Jackson, M. P., and Trudgill, B. D., 1999, Salt-related fault families and fault welds in the
633 northern Gulf of Mexico: AAPG bulletin, v. 83, no. 9, p. 1454-1484.
634 Rowan, M. G., Peel, F. J. and Vendeville, B. C., 2004, Gravity-Driven Fold Belts on Passive Margins. *in*
635 McClay K.R. ed., Thrust tectonics and hydrocarbon systems: *AAPG Memoir* **82**, 157-182.
636 Rowan, M. G., 2014, Passive-margin salt basins: hyperextension, evaporite deposition, and salt tectonics:
637 Basin Research, v. 26, no. 1, p. 154-182.
638 Rowan, M. G., 2018, The South Atlantic and Gulf of Mexico salt basins: crustal thinning, subsidence and
639 accommodation for salt and presalt strata: Geological Society, London, Special Publications, v. 476, p.
640 SP476.476.
641 Sawyer, D.S., Buffler, R.T. and Pilger Jr, R.H., 1991. The crust under the Gulf of Mexico Basin. Salvador
642 A. (ed), The Gulf of Mexico basin. The Geology of North America. Geological Society of America,
643 Boulder, Colorado: vol J, pp.53-72.
644 Salvador, A., 1987, Late Triassic-Jurassic paleogeography and origin of Gulf of Mexico basin: AAPG
645 Bulletin, v. 71, no. 4, p. 419-451.
646 Schultz-Ela, D.D., 2001. Excursus on gravity gliding and gravity spreading. Journal of Structural Geology,
647 23(5), pp.725-731.
648 Steffens, G. S., Biegert, E. K., Summer, H. S., and Bird, D., 2003, Quantitative bathymetric analyses of
649 selected deepwater siliciclastic margins: receiving basin configurations for deepwater fan systems:
650 Marine and Petroleum Geology, v. 20, no. 6, p. 547 - 561.
651 Worrall, D.M. and Snelson, S., 1989. Evolution of the northern Gulf of Mexico. *The geology of North*
652 *America; an overview: Geological Society of America, v. A*, pp.97-138.
653 Wu, S., Vail, P.R. and Cramez, C., 1990a. Allochthonous salt, structure and stratigraphy of the north-
654 eastern Gulf of Mexico. Part I: Stratigraphy. *Marine and Petroleum Geology*, *7*(4), pp.318-333.
655 Wu, S., Bally, A.W. and Cramez, C., 1990b. Allochthonous salt, structure and stratigraphy of the north-
656 eastern Gulf of Mexico. Part II: Structure. *Marine and Petroleum Geology*, *7*(4), pp.334-370
657

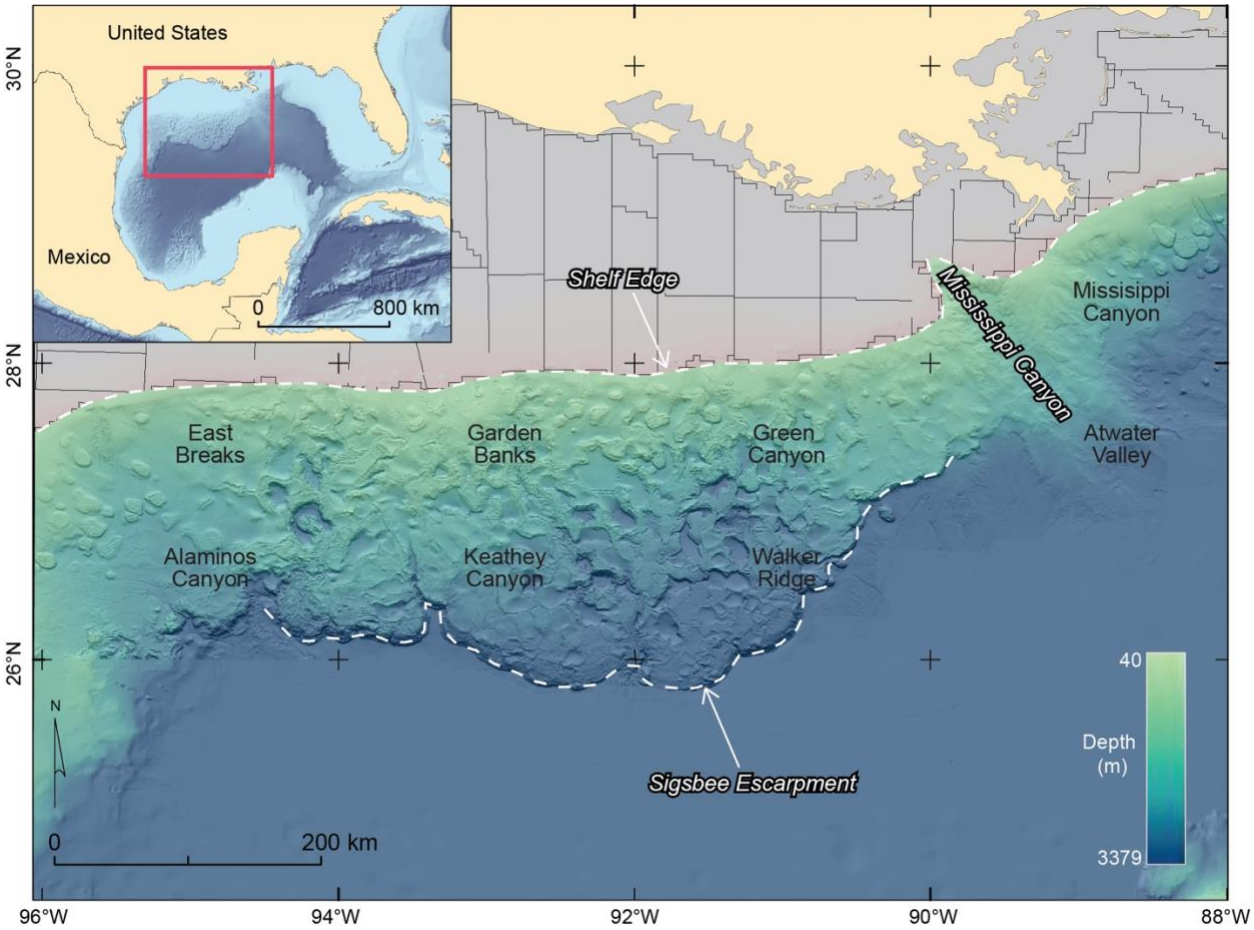

Figure 1. Seafloor bathymetry map of the Northern Gulf of Mexico, where the study area is located. Exact location cannot be released due to confidentiality. The Sigsbee Escarpment and the Shelf Edge delimit the approximate extend of the Sigsbee salt canopy. Labelled polygons represent the main protraction areas of the northern Gulf of Mexico slope. Bathymetry map is a combination of data from the BOEM and NOAA.

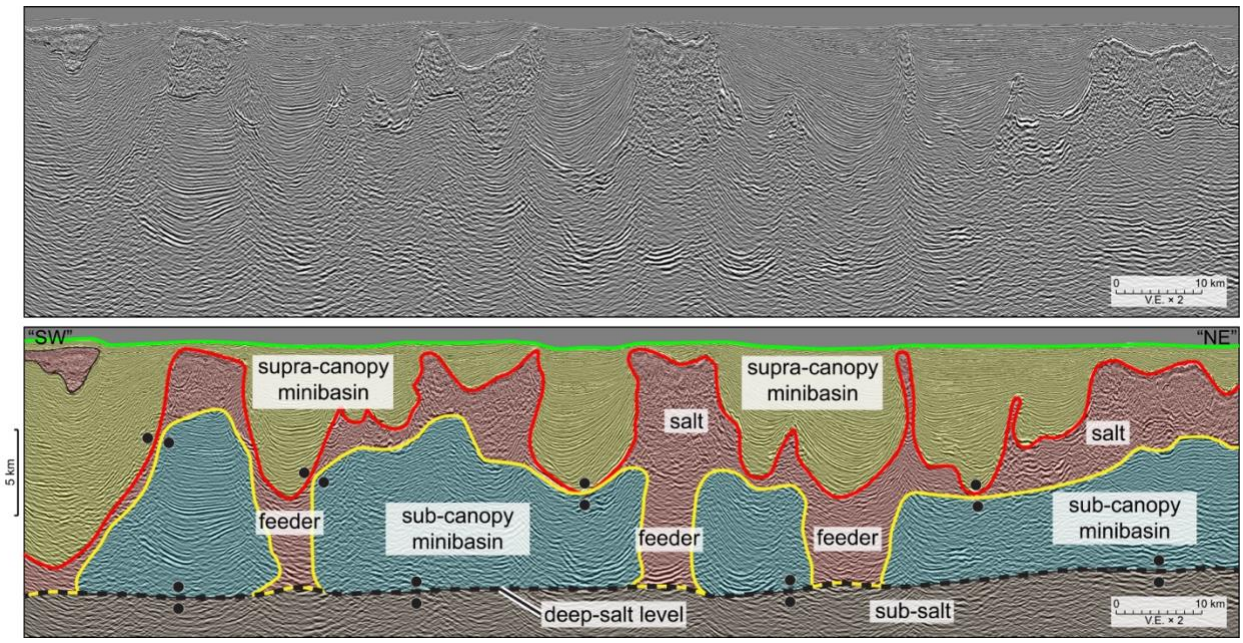

Figure 2. Uninterpreted (a) and interpreted (b) seismic section across the study area to illustrate the different structural elements discussed throughout the text. The four mapped horizons are highlighted: seafloor (green), top Sigsbee Canopy surface (corresponding to the base of supra-canopy minibasins) (red), base Sigsbee Canopy surface (also referred to as base-of-salt in the text) (yellow) and deep salt level with undifferentiated autochthonous and allochthonous salt (dashed black line). The feeders are the vertical conduits that connect the two salt levels.

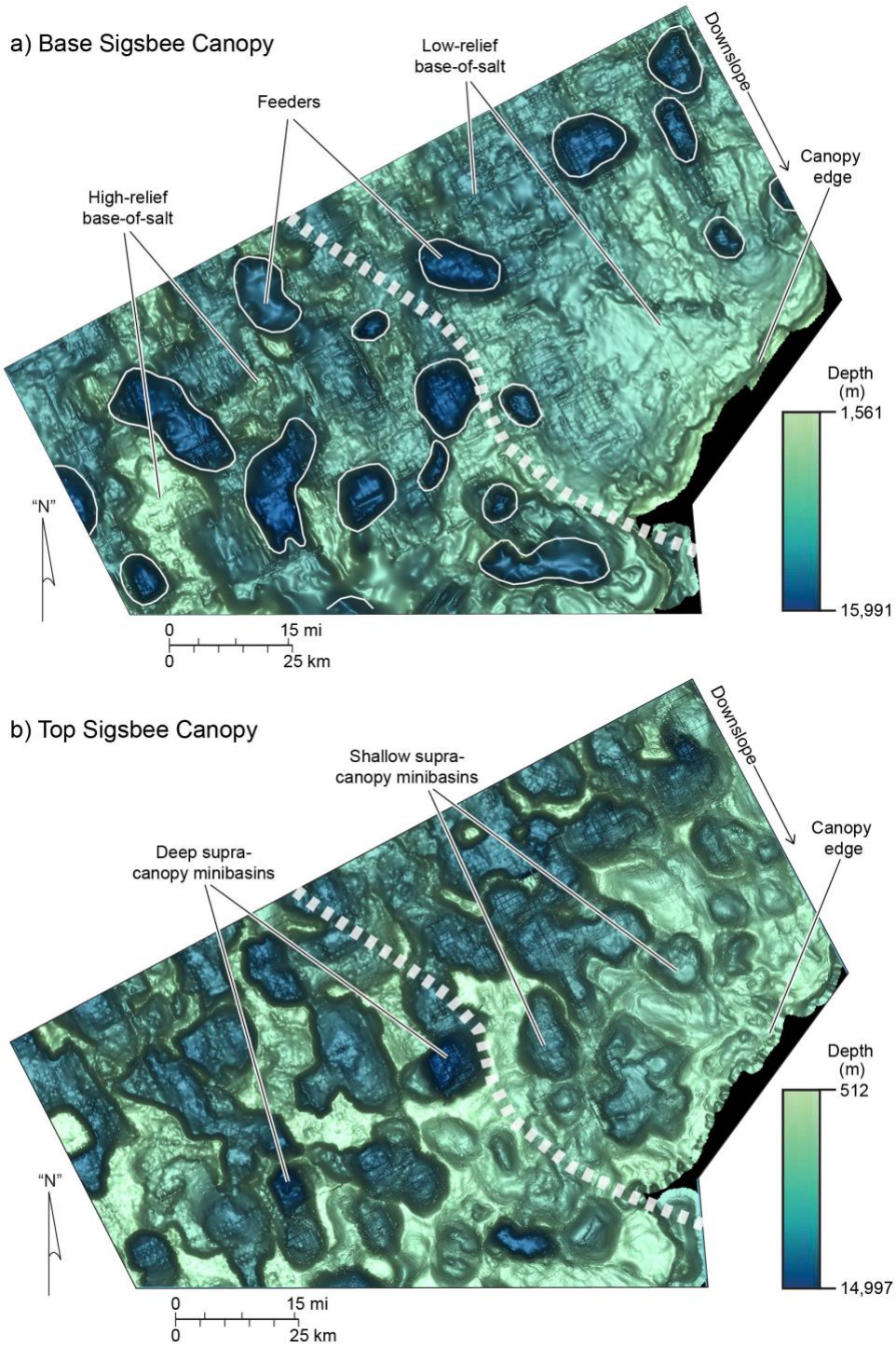

Figure 3. a) Map view of base Sigsbee Canopy surface, where the marked structural lows represent feeders that connect the deep and shallow salt levels. b) Map view of top Sigsbee Canopy, where each structural low represents a minibasin hat has subsided into the salt canopy. Maps have been rotated and are oriented according to a false North due to confidentiality. The dashed line indicates the approximate boundary between the two structural domains that are described in the text.

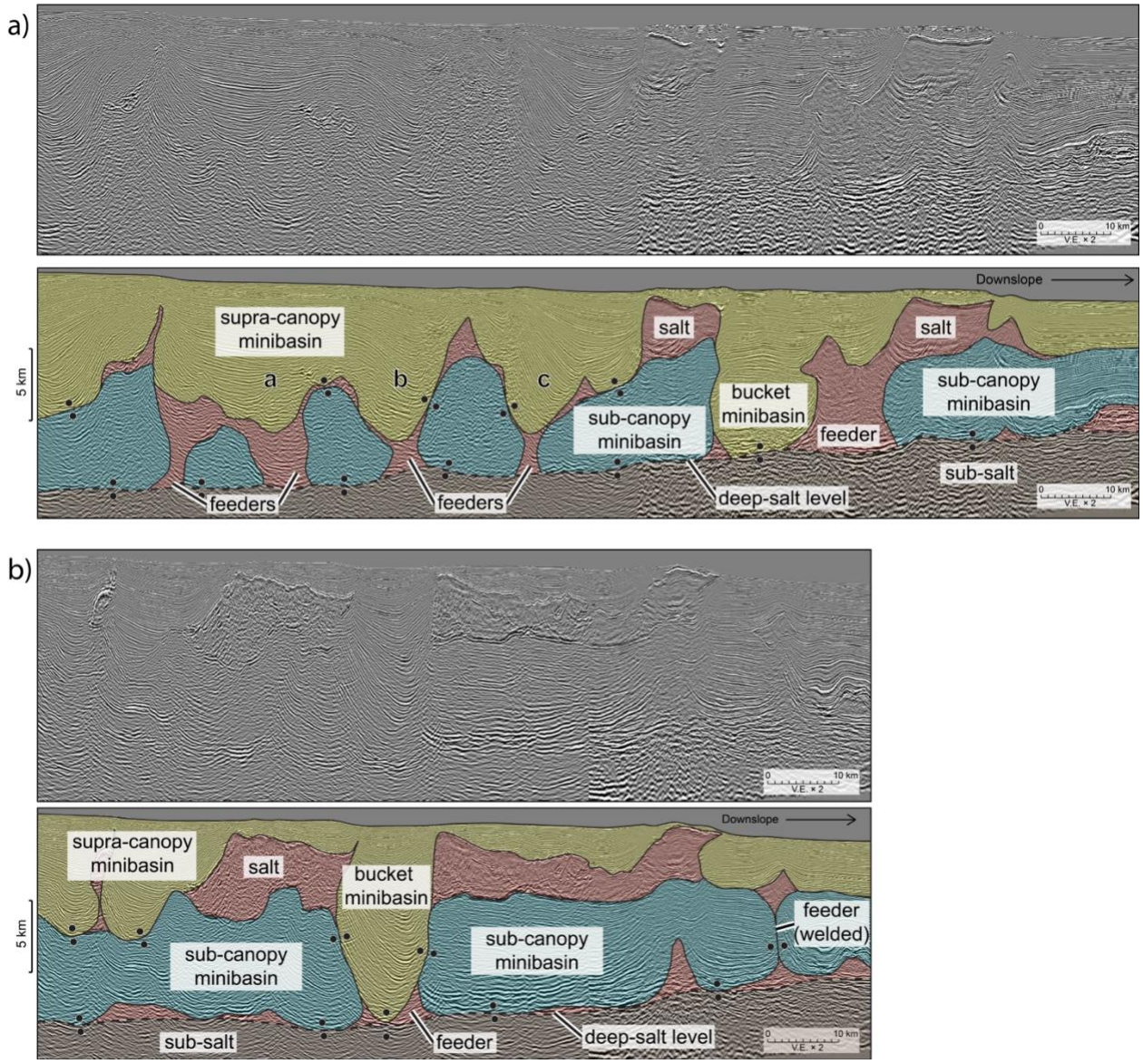

Figure 4. Uninterpreted and interpreted seismic sections across the "Southwest" domain. Both sections show a landward dipping deep salt level. Sub-canopy primary sequence is very rugose and discontinuous with many feeders connecting the deep salt and canopy salt levels. Feeders are abundant, especially in a). Feeders range in height and wide but most of them, contain a bucket minibasin inside. Bucket minibasins can be partially filling the feeder, or completely filling the feeder and welded to the deep salt level inside the feeder. Overall, the contact area between the sub-canopy and supra-canopy sequences is very rugose and sinuous.

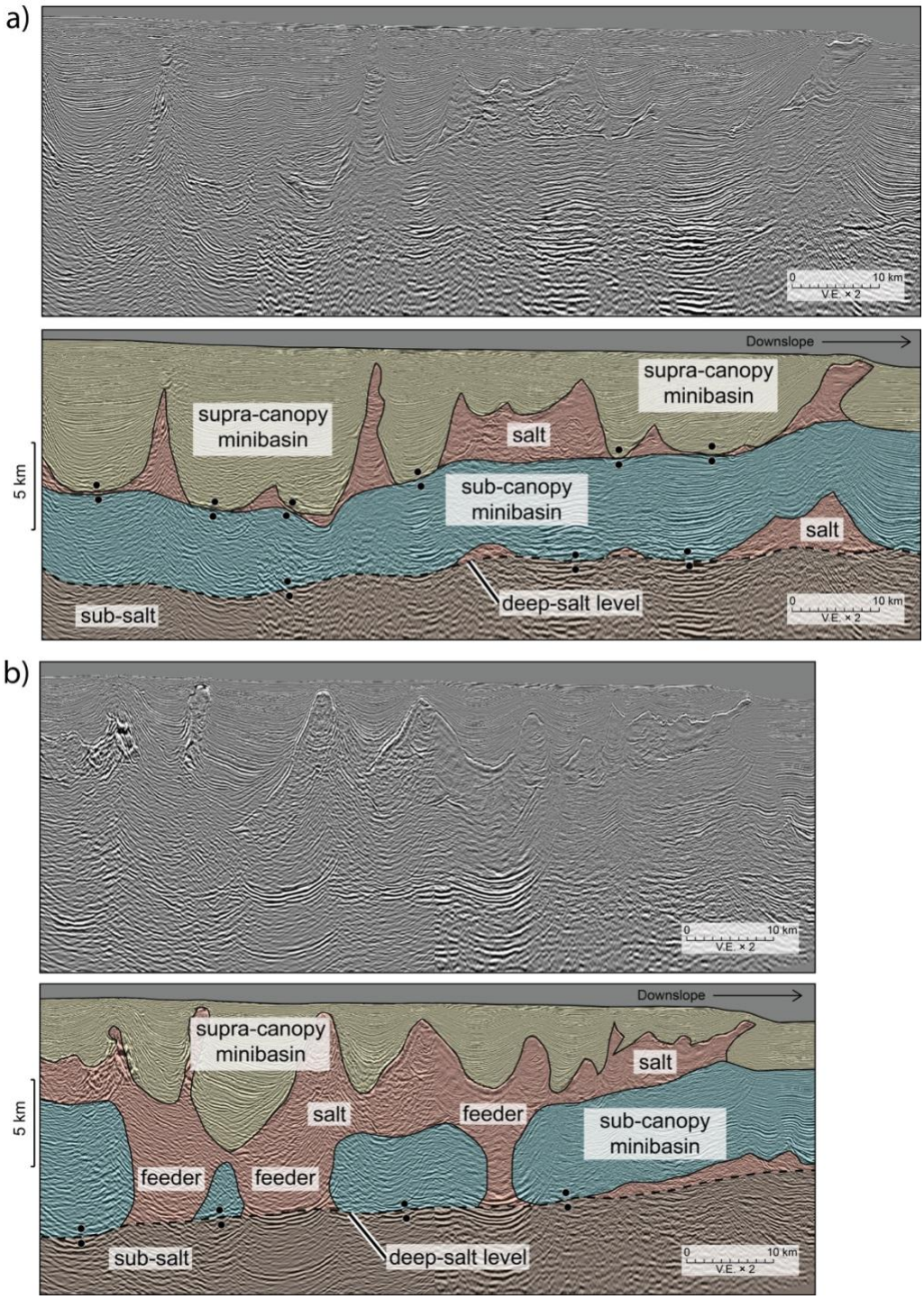

Figure 5. Uninterpreted and interpreted seismic sections across the "Northeast" domain. Both sections show a landward dipping deep salt level. In section a), the sub-canopy sequence is very continuous and relatively smooth flat portions, except for areas where the slope of the surface changes. The supra-canopy minibasins on top are welded to the smooth sub-canopy sequence. In section b) the sub-canopy is discontinuous with various feeders connecting the shallow and deep salt levels. Supra-canopy minibasins on top are relatively thin and do not weld to the sub-canopy sequence. Overall, section a) illustrates a relatively smooth contact surface between supra- and sub-canopy sequence, while section b) illustrates and area where there is no contact surface between sub- and supra-canopy sequences.

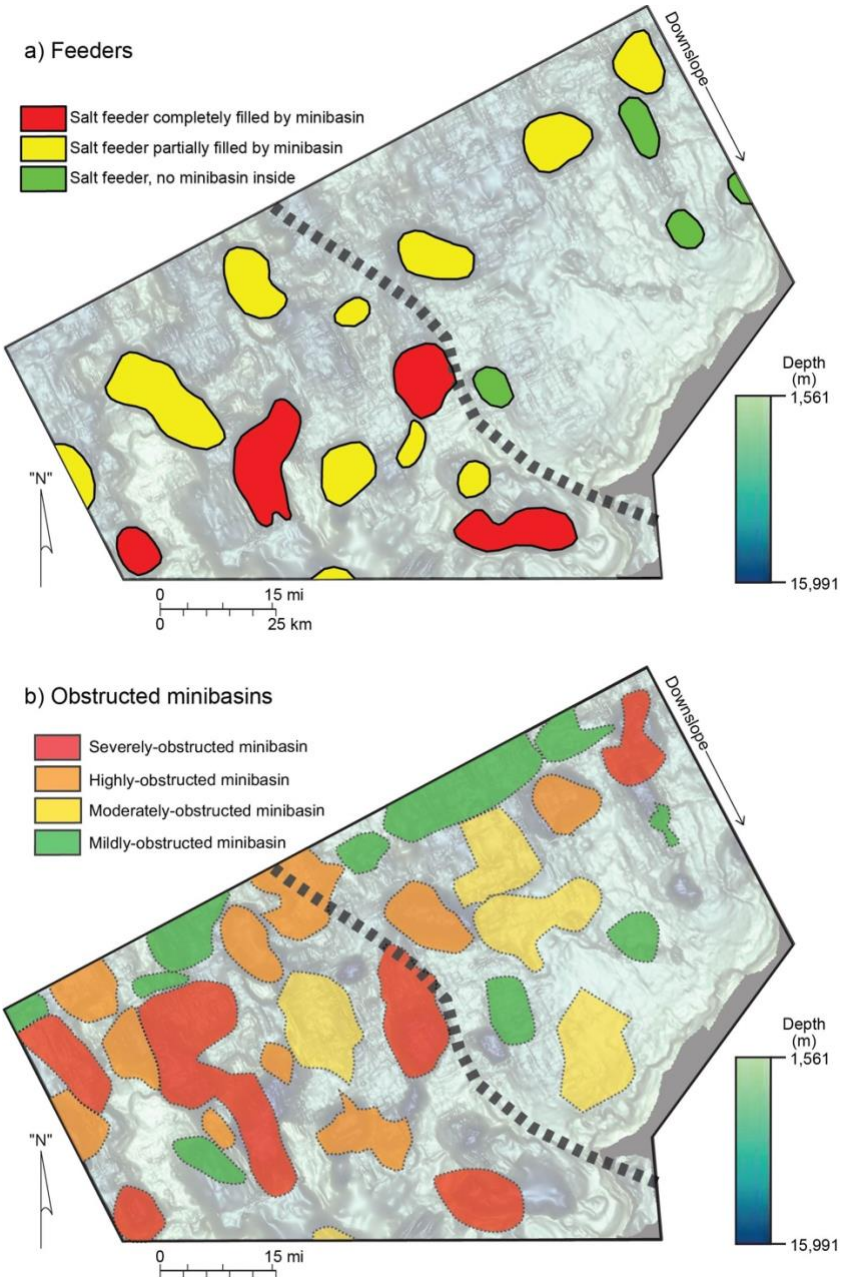

Figure 6. a) Map view showing the outlines of feeders interpreted in the study area. Feeders are colored depending on whether they are completely or partially filled with a supra-canopy minibasin inside, or whether they do not have a supra-canopy minibasin inside. Notice the absence of feeders completely filled with minibasins inside in the "Northeast" domain, as well as the absence of empty feeders in the "Southwest" domain. Dashed black line represents hypothetical boundary between "Northeast" and "Southwest" domains. Background map corresponds to the Base of Sigsbee Canopy horizon (Fig. 3a). b) Map view showing the outlines of obstructed minibasins colored according to severity of obstruction (from Duffy et al., 2019). Notice the abundance of obstructions classified as severe or highly obstructed in the "Southwest" domain, as compared to the "Northeast" domain. Background map corresponds to the Base of Sigsbee Canopy horizon (Fig. 3a). The dashed line indicates the approximate boundary between the two structural domains that are described in the text.

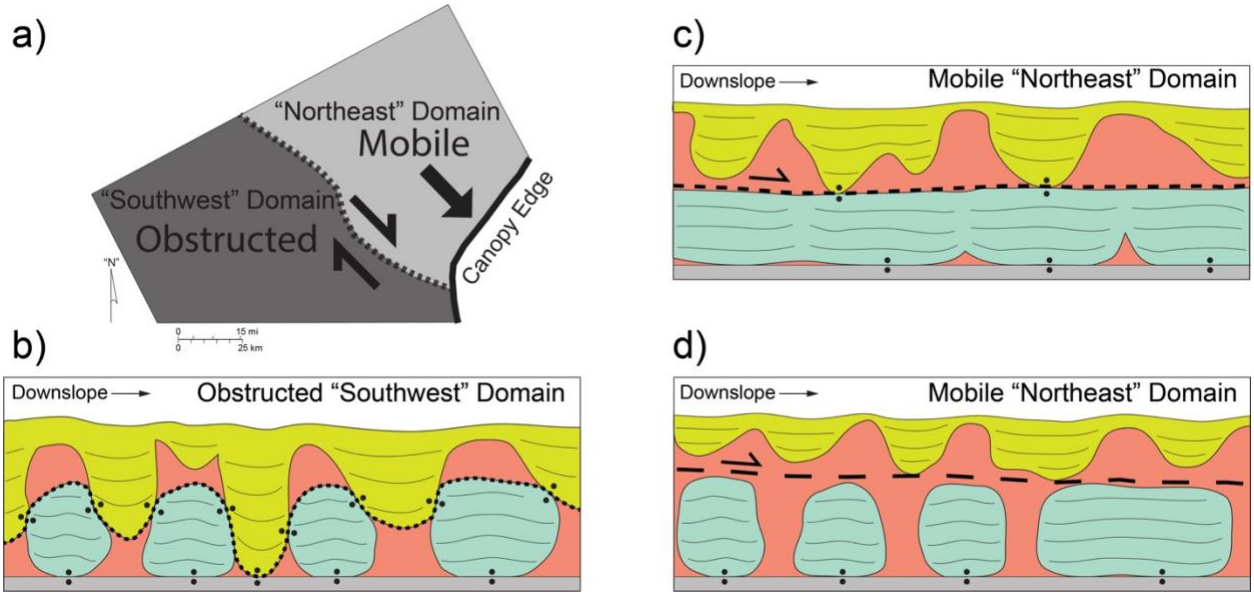

Figure 7. a) Map view of the outline of the study area and the approximate boundary between the two differentiated domains: the "Northeast" mobile domain, and the "Southwest" obstructed domain. The differential potential for mobility would result in a dextral strike-slip boundary. b), c) and d) Synoptic sections of the different structural styles observed in the study area. b) Synoptic section synthesizing the elements observed in the seismic sections of the Western domain area: abundant and prominent feeders that are completely or partially infilled with supra-canopy minibasins. There is not a clear detachment surface between the supra-canopy cover and the sub-canopy sequence, but rather a sinuous and irregular contact surface defined by the abundant welds. c) Synoptic section of the "Northeast" domain where the base of shallow salt has very low relief, with supra-canopy minibasins above welded or not welded on top of the sub-canopy sequence. d) Synoptic section of the "Northeast" domain where base of shallow salt has very high relief, with abundant feeder (smaller than in the West), but supra-canopy minibasins might not always be welded or sunk into the feeders. In c) and d) examples, there is a potential detachment surface between the supra-canopy cover and the underlying sub-canopy sequence.

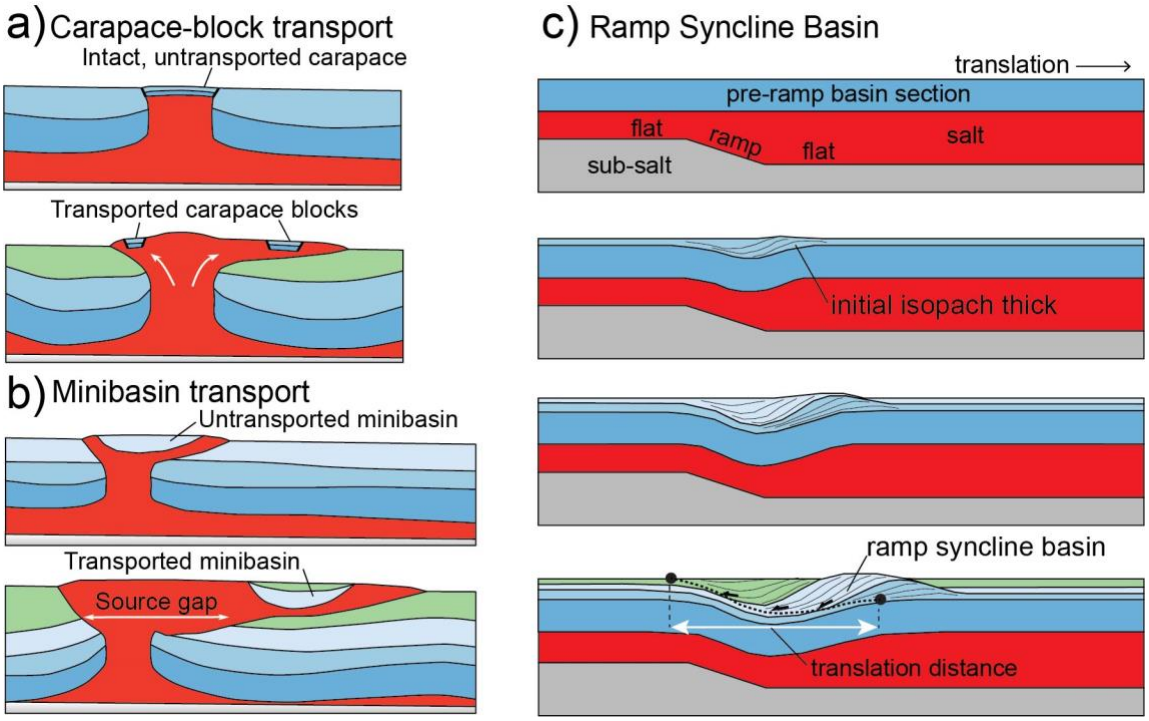

Figure 8. Schematic cartoons of lines of evidence for identifying large-magnitude transport of advancing salt canopies. (a) and (b). Schematic restorations of transport and emplacement of a carapace of two types of roof material: (a) carapace-blocks and (b) entire minibasins (modified from Jackson and Hudec, 2018). Note that in both cases, the transport of roof material with the advancing sheet has placed the older sediments contained in the carapace or in the minibasin directly above the younger sediments in the sub-canopy section. Identifying the source gap from where the roof material was originated can provide estimates of the transport distance. (c) Evolutionary model of a salt-detached ramp syncline formation (from Pichel et al., 2018). The ramp syncline basin forms by translation of the sedimentary cover over a salt layer. As the cover is translated over the base salt ramp, new accommodation space is created on top. Translation movement is recorded by the onlap offset. Distance between oldest and youngest ramp-related onlaps provide estimates for the transport distance.

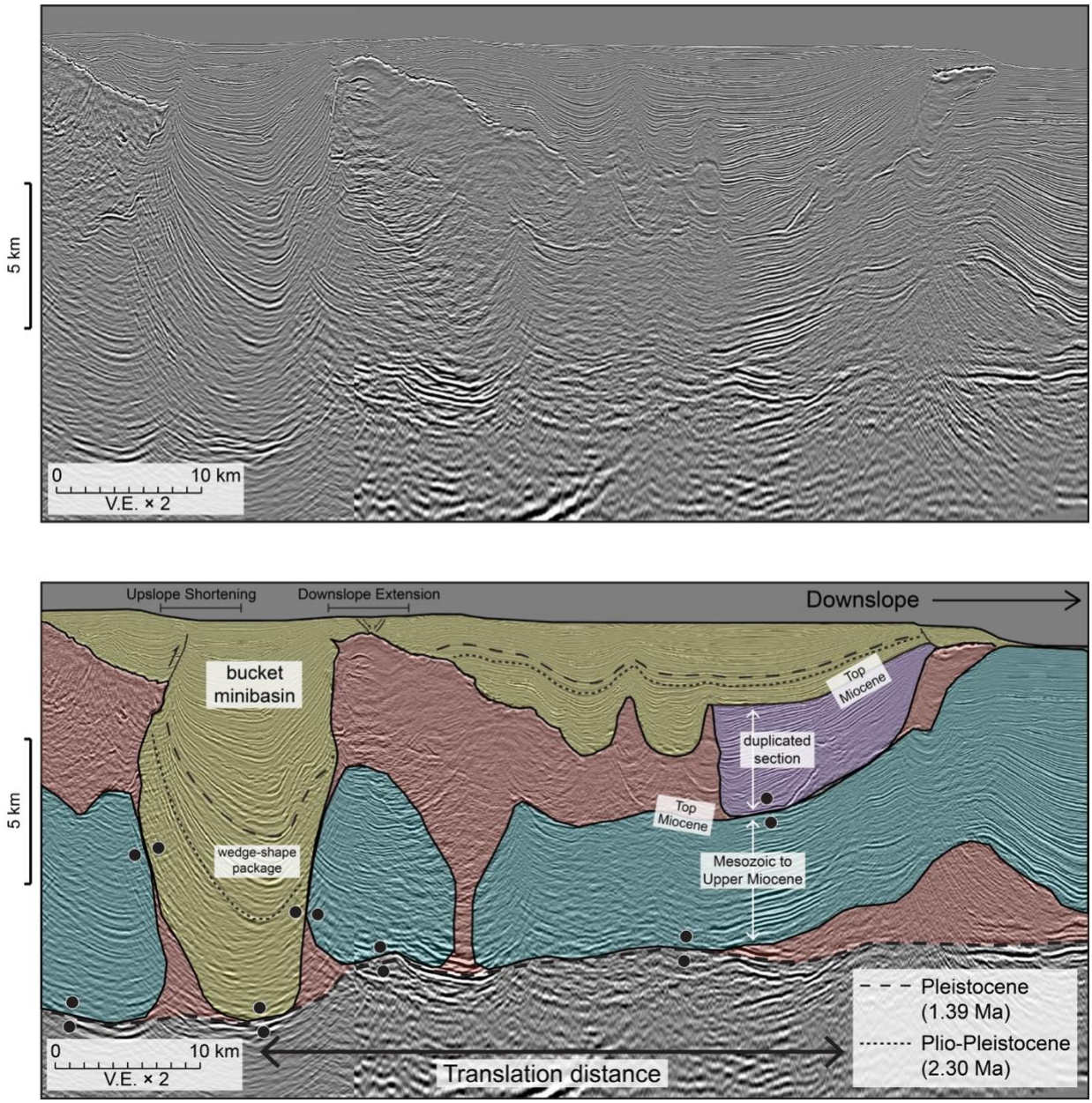

Figure 9. Uninterpreted and interpreted seismic section across a far-travelled minibasin and its probable source area (feeder) upslope. The minibasin contains older stratigraphic section of sediments at its base that are directly above sub-canopy primary sequence sediments of younger age, thus the minibasin contains a duplicated section. The minibasin is interpreted as a rafted or far-travelled minibasin source from a feeder located several tens of kilometers up-dip which at present-day is occupied by a bucket minibasin. Ages are based on GBDS surface picks of biostratigraphy markers from wells in the study area.

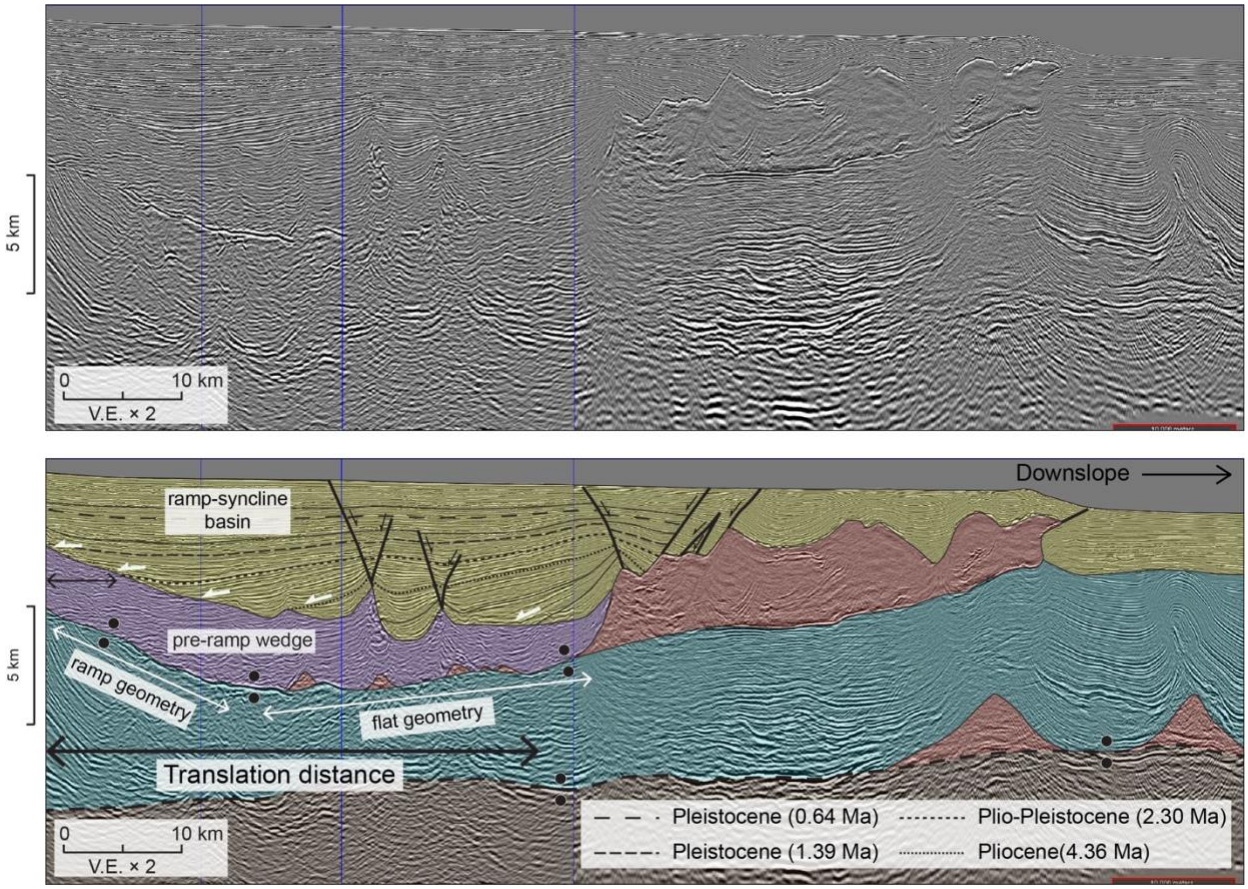

Figure 10. Uninterpreted and interpreted seismic section across a ramp syncline basin in the study area. The minibasin contains a broadly constant thickness basal section (pre-ramp wedge) and an overlying synclinal section with onlaps (white arrows) prograding updip in the section. The basin is interpreted as a ramp-syncline basin formed in relation with the ramp-flat geometry of the sub-canopy (primary) topography. The present-day distance from the oldest onlap to the updip location of the flat-to-ramp transition (not seen in the section) gives an estimate of the transport distance of several tens of kilometers. Ages are based on GBDS surface picks of biostratigraphy markers from wells in the study area.

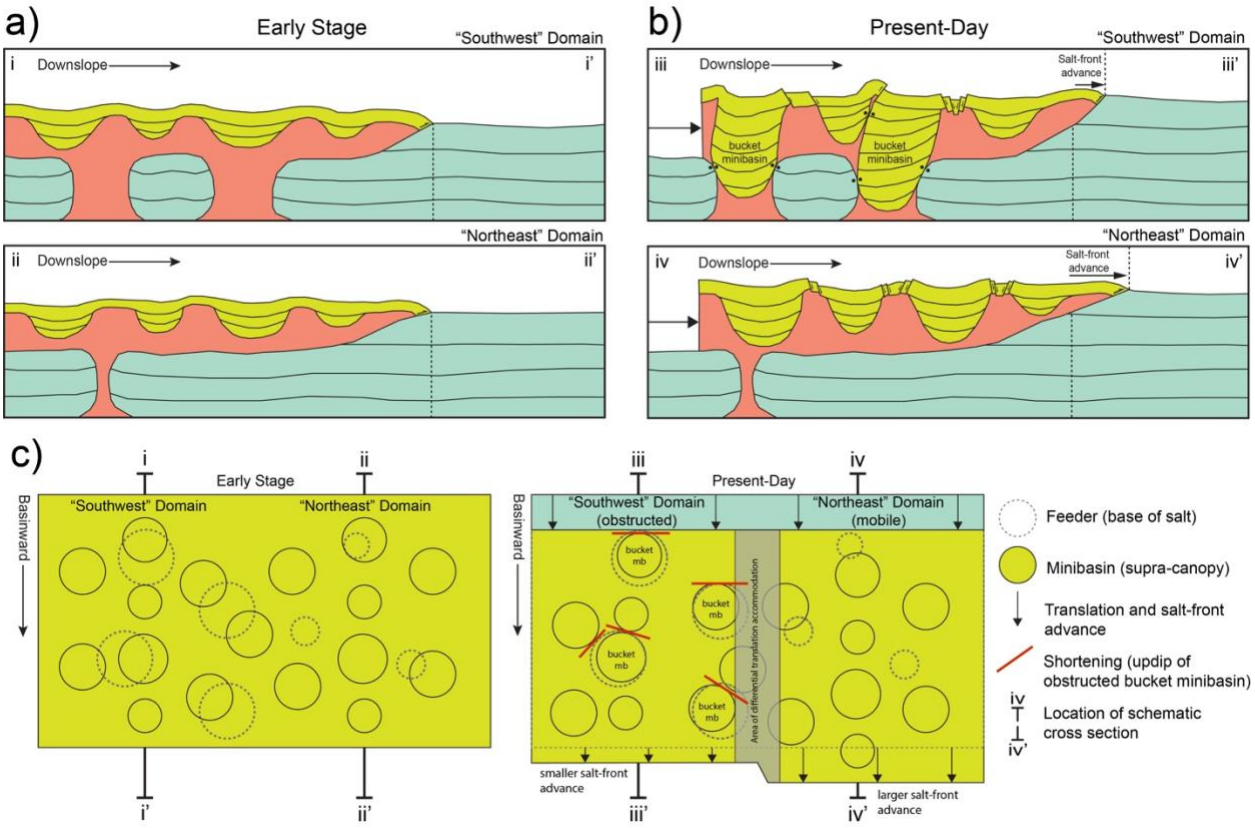

Figure 11. (a)- (b). Synoptic cross section sketches illustrating the evolution of the "Southwest" Domain and the "Northeast" Domain, from an early stage (both domains are mobile) to a late stage, where the "Southwest" Domain is obstructed and the "Northeast" Domain is still mobile. c) Synoptic plan-view sketch illustrating the differential evolution between the two domains. The obstruction of the "Southwest" Domain and subsequent continuous translation of the "Northeast" Domain results in differential salt advance in the front. A broad area is delimited in between the two domains, where the differential translation needs to be accommodated. Deformation can be accommodated in a diffuse way (e.g. short fault segments along minibasin boundaries as opposed to a large linear strike-slip fault).

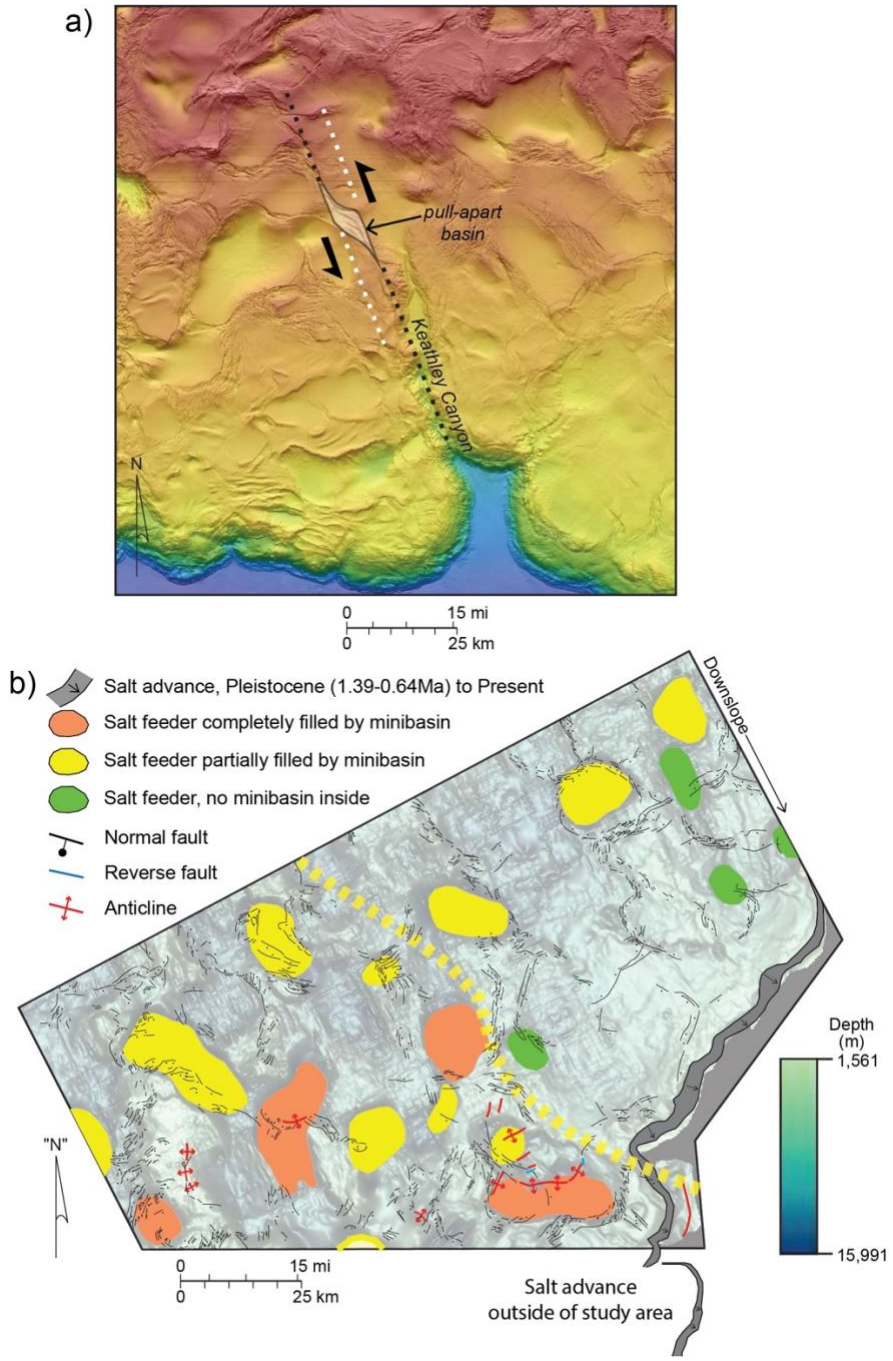

Figure 12. a) Seafloor map of the west of Sigsbee canopy showing a long and straight left-lateral strike slip zone in Keathley Canyon (after Dooley and Schreurs, 2012) associated to differential downslope translation of the Sigsbee canopy. b) Map of structures observed in the seafloor of the study area. Background map corresponds to the Base of Sigsbee Canopy horizon (Fig. 3a). Notice that most widespread structures correspond to faults grouped in deformation zones along minibasin boundaries (e.g. grabens) indicating a major component of stretching. Shortening structures (reverse faults and folds) are limited to the "Southwest" domain. No clear long and straight right-lateral strike slip deformation zone is observed in the seafloor along the boundary (yellow dashed line) between the two domains. However, Pleistocene to Present-Day differential salt advance is indicated by the interpretation of sub-canopy salt cutoffs, with higher advance occurring at the "Northeast" domain.